

Interaction between Casein and the Oppositely Charged Surfactant

Yan Liu and Rong Guo*

College of Chemistry and Chemical Engineering, Yangzhou University, Yangzhou, 225002, People's Republic of China

Received April 6, 2007

The interactions between the classical cationic surfactant dodecyltrimethylammonium bromide (DTAB) and 2.0 mg/mL casein were investigated using isothermal titration calorimetry (ITC), turbidity, dynamic light scattering (DLS), and fluorescence spectra measurements. The results suggest that the cationic headgroup of the surfactant individually binds to the negatively charged amino acid sites on the casein chains because of the electrostatic attraction upon the addition of DTAB. When the surfactant concentration reaches a critical value c_1 , DTAB forms micelle-like aggregates on the casein chain, resulting in the formation of insoluble casein/DTAB complexes. Further addition of DTAB leads to the redissolution of casein/DTAB complexes because of the net positive charge on casein/DTAB complexes and the formation of DTAB free micelles. The addition of salt screens the repulsion between the surfactant headgroups and the attraction between casein and surfactant molecules, which weakens the binding of surfactant onto the casein chain, favoring the formation of free surfactant micelles.

Introduction

Interactions between natural (or synthetic) polymers and surfactants in aqueous solutions have attracted much interest because of their widespread applications and relatively complex behaviors.^{1–7} Surfactant–polymer mixtures may associate into different nanostructures, which can be designed by simply changing the composition of the species in the system. As a result of the capability to form new nanostructures, numerous research groups have devoted their attention to advancing the fundamental understanding of the physics governing these interactions.^{8–14} In those studies, various techniques have been applied to the study of the surfactant–polyelectrolyte interaction, including surface tension,^{8,9} viscosity,¹⁰ zeta potential methods,¹¹ fluorescence spectroscopy,¹² isothermal titration calorimetry (ITC),¹³ and dynamic light scattering (DLS).¹⁴ Among these techniques, ITC has been increasingly employed during the past years. Its high sensitivity allows the precise determination of the parameters normally used to characterize polymer–surfactant interactions.¹³

Casein has been widely used in the formulations of food, cosmetics, and some other consumer products. The casein constituents, α_{s1} -, α_{s2} -, β -, and κ -casein, exist in proportions of approximately 4:1:4:1 by weight, and the average pI of casein is 4.8. As an approximation, the caseins can be thought of as block copolymers consisting of blocks with high levels of hydrophobic or hydrophilic amino acid residues. Therefore, caseins can form casein micelles via a balance of attractive hydrophobic interactions and electrostatic repulsion in aqueous solution.^{15–18}

The property of casein micelles is largely determined by the structure of the micelle. The extreme stability of the casein micelles derives from the layer or brush of κ -casein molecules, extending their C-terminal part into the solution. If the brush were not dense enough, or were collapsed on the surface, the

steric stabilization would be absent, leading to flocculation. Many studies have shown that additives can significantly alter the behavior and overall performance of casein.^{19–23}

In commercial food and cosmetic products containing casein, the addition of surfactant is generally employed to obtain better performance for the products. To contribute to a better understanding of the forces involved in the surfactant–casein interaction, in this article, we present a study on the interaction between casein micelles and the oppositely charged surfactant dodecyltrimethylammonium bromide (DTAB), employing isothermal titration calorimetry (ITC), turbidity, dynamic light scattering (DLS), and fluorescence techniques. The results provide detailed information on the structure–property relationship of casein micelles modulated by the oppositely charged surfactant, which will broaden the application range of casein in food, cosmetic, and medical applications.

Materials and Methods

Materials. Casein was purchased from Sigma (90%). Dodecyltrimethylammonium bromide (DTAB, purity >99%) from Aldrich was recrystallized twice before use. Pyrene and 1-anilino naphthalene-8-sulfonate (ANS) (99%) were obtained from Aldrich. All samples were prepared in 5 mM sodium phosphate buffer of ionic strength 0.01 mol/L at pH 6.8. Casein concentration was kept at 2.0 mg/mL. (The critical micellar concentration of casein under experiment conditions is about 1.0 mg/mL.) Therefore, the casein micelles were in a dynamic equilibrium with submicelles and monomers in solution. The casein solutions were filtered through a Millipore filter with a 2.0 μ m pore size and thermostated at 25 °C for at least 0.5 h before use. All other reagents used were of analytical grade, and water was triply distilled.

Microcalorimetry. Heats of dilution were measured using a VP–ITC titration microcalorimeter from MicroCal Inc., Northampton, MA at (25 ± 0.1) kJ mol^{–1}. Experiments were carried out titrating the micellar surfactant first into buffer and then into an aqueous solution containing 2.0 mg/mL casein. In a typical experiment, the casein solution was placed in the 1.438 cm³ sample cell of the calorimeter, and DTAB solution was loaded into the injection syringe. Both solutions were prepared in phosphate buffer and were degassed before use. The

* To whom correspondence should be addressed. E-mail: guorong@yzu.edu.cn.

pH of solutions has been checked to be constant in the studied surfactant concentration range; therefore, pH has no effect on the ITC data. The reference cell was filled with deionized water. DTAB solution was titrated into the sample cell as a sequence of 50 injections of 5×10^{-6} dm³ aliquots. The duration of each injection was 10 s, and the time delay (to allow equilibration) between successive injections was 240 s. The contents of the sample cell were stirred throughout the experiment at 307 rpm to ensure thorough mixing. Raw data were obtained as a plot of heating rate ($\mu\text{cal s}^{-1}$) against time (min). These raw data were then integrated to obtain a plot of observed enthalpy change per mole of injected DTAB (ΔH_{obs} , kJ mol⁻¹) against DTAB concentration (mM). Control experiments included the titration of DTAB into buffer, buffer into casein, and buffer into buffer. The last two controls resulted in small and equal enthalpy changes for each successive injection of buffer and, therefore, will not be considered further in data analysis. The titration of DTAB into buffer yielded enthalpy changes that will be discussed later.

Turbidity Measurements. Turbidity measurements were carried out with a Shimadzu 1601 PC UV/vis spectrometer. The turbidity of the surfactant/casein mixed solutions was monitored by the transmittance at 450 nm. A cuvette with 1 cm pathway was used. All of the measurements were conducted at $(25 \pm 0.1)^\circ\text{C}$.

Dynamic Light Scattering (DLS). Dynamic light scattering measurements were made at $25.0 \pm 0.1^\circ\text{C}$ and at a scattering angle of 90° to the incident beam, using an ALV 5022 laser light-scattering instrument equipped with a 22 mW He-Ne laser at 632 nm (JDS model 1145P) in combination with an ALV-5000 digital correlator with a sampling time range of 1.0 μs to 1000 ms. The duration of each experiment was in the range of 5–10 min, and each experiment was repeated two or more times.

Steady-State Fluorescence. Steady-state fluorescence experiments were performed with an RF-5301 luminiscence spectrometer (Japan Shimadzu Company) equipped with a thermostated water-circulating bath. During the experiments for casein solution, the excitation and emission slits were fixed at 3.0 and 1.5 nm, respectively, the excitation wavelength was set at 295 nm, and the emission spectra were collected from 300 to 500 nm. In all of the measurements, the scan rate was selected at 240 nm/min.

Pyrene was used as the probe to determine the microenvironmental polarity of casein micelles by observing its fluorescence fine structure. The emission spectra were measured in the wavelength range of 350–600 nm with the excitation wavelength being 338 nm. The pyrene concentration was 1.0×10^{-6} M.

ANS was used as the anionic probe to determine the property of casein micelles. The emission spectra were measured in the wavelength range of 400–560 nm with the excitation wavelength being 380 nm. The ANS concentration was 1.0×10^{-5} M.

Results and Discussion

Thermodynamics of the Binding of DTAB to Casein. ITC is one of the most sensitive techniques that permits the direct measurement of thermodynamic changes in the course of binding and micellization.^{24,25} Figure 1A shows the isothermal titration curve (■) of 0.2 M DTAB in 2.0 mg/mL casein solution together with the dilution curve (□) of DTAB in buffer. A large deviation between these two titration thermograms is evident. The difference is attributed to the interactions between DTAB and casein. Since the heat of demicellization effects are not mirrored in the casein–surfactant binding experiments, the ITC data shown in this article have not been corrected by subtraction of the DTAB–buffer control.

The titration of the micellized DTAB into buffer leads to the observation of an inflection in the ITC isotherm plot of molar enthalpy change against DTAB concentration (Figure 1A). The position of this inflection corresponds to the critical micellar

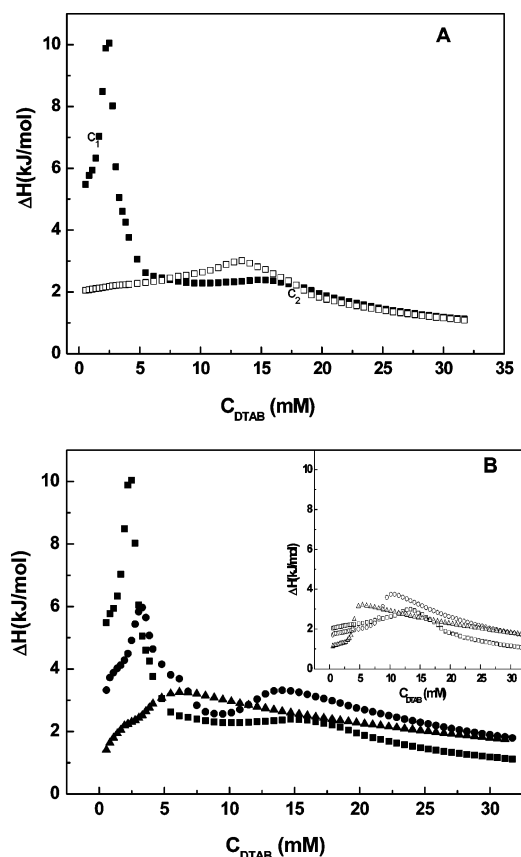


Figure 1. (A) ITC curves for titrating 0.2 M DTAB in 2.0 mg/mL casein solution (■) and buffer solution (□) at 298 K. (B) ITC curves for titrating 0.2 M DTAB in 2.0 mg/mL casein solution with added 0 M (■), 0.1 M (●), and 0.5 M (▲) NaCl, together with the dilution curves in buffer solution with added 0 M (□), 0.1 M (○), and 0.5 M (△) NaCl (insert).

concentration (cmc) for DTAB under the conditions of this study. The initial enthalpic responses are endothermic and are due to the demicellization that occurs upon dilution of the titrated DTAB micellar solution in the calorimetry cell. At the point of inflection, the cell solution concentration reaches the cmc of the surfactant, and demicellization no longer occurs. For DTAB, the cmc occurs at a concentration of approximately 14 mM in the buffer, which is smaller than that in pure water (18.0 mM).

The large endothermic deviation between the titrations at low DTAB concentration in Figure 1A indicates that the interaction between the surfactant and casein occurs even at the lowest DTAB concentration measured, 0.55 mM. In oppositely charged polymer/surfactant systems, ionic surfactant monomers bind to the charged sites of the polymer backbone prior to the formation of micelle-like aggregates on the polymer chains. Casein molecules are negatively charged under physiological conditions at pH 6.7. At the beginning of the titration, the added DTAB micelles from the injection syringe break up into DTAB monomers, and the DTAB monomers are further diluted in casein solution and then bind to negatively charged sites on the casein micelle shell through electrostatic attraction, which results in an increase in ΔH_{obs} in the initial part of the titration curves. Obviously, DTAB monomers can also bind to the negatively charged sites on casein monomers (or casein submicelles) through electrostatic attraction.

At a certain surfactant concentration, ca. 1.4 mM, as shown in Figure 1A, a sudden increase in the enthalpy of titration in casein solutions is observed. This is associated with the cooperative formation of small surfactant aggregates around

casein chains. This concentration is called the critical aggregation concentration (c_1), which is much lower than the cmc of DTAB in water.

The observed increase in enthalpy, with respect to the reference curve for the surfactant dilution in water, is associated with the casein chain dehydration caused by surfactant binding.^{26–28} As surfactant binding progresses, ΔH_{obs} reaches a maximum and then decreases as the surfactant concentration increases. This decrease in the enthalpy difference suggests a smaller extent of casein dehydration upon surfactant binding, which continues until the reaction passes through a minimum c' (in the case represented in Figure 1, at ca. 10 mM), followed by a very small increase in enthalpy until the two dilution curves merge. Therefore, this merging point (at ca. 18 mM) represents the concentration after which the formation of free micelles becomes more favorable and is usually referred to as c_2 , the second critical or saturation concentration. At higher concentrations, only the dilution of DTAB micelles takes place.

To further understand the casein/DTAB complex formation, isothermal titration microcalorimetry has been used to characterize the formation of casein/DTAB complexes in the presence of 0.10 and 0.50 M NaCl. The enthalpy binding curves obtained from titrating 0.2 M DTAB into 2.0 mg/mL casein solutions containing 0, 0.1, and 0.5 M NaCl (given by filled symbols) are plotted in Figure 1B, together with the dilution curves of DTAB into buffer containing identical amounts of NaCl (given by open symbols in the insert figure in Figure 1B). The distinct endothermic peak detected in the dilution curves characterizes the cmc of DTAB under different salt conditions. It is found that cmc decreases from 14 to 6 mM when the NaCl concentration increases to 0.5 M since micellization is favored by the additional salt that screens the electrostatic repulsion between the surfactant headgroups.

In the presence of 0.1 M NaCl, the binding isotherm exhibits almost the same profile as that in the absence of salt. However, c_1 increases from 1.1 to 1.9 mM, and c_2 decreases from 18 to 14.6 mM. Obviously, the addition of salt screens the electrostatic attraction between the oppositely charged amino acid residues in casein and the polar head of DTAB, which weakens the binding of DTAB molecules to the casein, resulting in the increase of c_1 . However, the addition of salt screens the electrostatic repulsion between the surfactant headgroups, which favors the formation of free micelles, and hence a lower c_2 .

When the NaCl concentration is increased to 0.5 M, the profile of the binding isotherms is greatly altered, almost coinciding with the curves of DTAB into buffer at the same NaCl concentration. The calorimetric titration curve does not give an endothermic peak for the complex formation. The slight deviation of the binding curve (shown by \blacktriangle) from the dilution curve (shown by \triangle) at low DTAB concentration characterizes the weak binding of DTAB to casein. Thereafter, the enthalpy curve is almost identical to the peak detected in the dilution curve and exhibits an endothermic peak at a DTAB concentration of 6 mM. This peak does not represent the micellization of casein-bound surfactant molecules but represents the formation of free micelles. In excess salt, where the electrostatic attractive force between casein and surfactant is considerably screened, electrostatic binding is significantly weakened, and consequently, the casein-induced micellization of surfactant cannot occur since very small amounts of surfactant are electrostatically bound to the casein chains. However, the electrostatic repulsion between the surfactant headgroups is also shielded by the addition of salt, which favors the formation of free micelles.

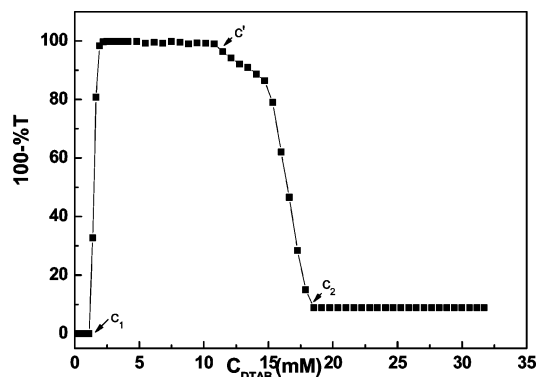


Figure 2. Turbidity 100-%T of casein (2.0 mg/mL) with DTAB as a function of C_{DTAB} .

Turbidity Analysis of Mixtures of Casein and DTAB.

Figure 2 shows turbidimetric titration curves of casein solution with DTAB. As shown in Figure 2, turbidity is constant and very small at a DTAB concentration lower than 1.4 mM, then increases sharply at a DTAB concentration higher than 1.4 mM, and then remains constant with the addition of DTAB. Beyond 11 mM, the turbidity decreases sharply to a small value and finally remains constant again when the DTAB concentration reaches 18 mM with the continuous increase of DTAB concentration. The point of the initial turbidity increase is designated as c_1 , that of the turbidity decrease is designated as c' , and the finally turbidity constant is designated as c_2 .

Because the abrupt change in turbidity arises mainly from the change of mass and size of aggregates in the solution, the above changes of turbidity are supposed to be the result of the formation and the redissolution of large casein /DTAB complexes. Here, the c_1 value corresponds to the critical DTAB concentration for the onset of surfactant aggregation formation on casein chains. Below c_1 , DTAB monomers bind to the negatively charged sites on the casein micelle. Although the net charge on the casein micelle surface has been reduced, the remaining net charge can still stabilize the casein micelle. Beyond c_1 , DTAB aggregates are formed at the shell of casein micelles, and insoluble casein/DTAB complexes are formed because of the marked electrical neutralization of the negative charge of casein micelles by cationic DTAB. This leads to the sharp increase in the turbidity of the system beyond c_1 . At the same time, the binding of DTAB on casein monomers (or submicelles) also leads to insoluble casein/DTAB complex formation.

After the turbidity maximum, larger casein/DTAB complexes begin to redissolve into smaller complexes at c' . Beyond c' , the net positive charges on the complexes due to the binding of more cationic surfactant molecules will lead to the redissolution of the large casein/DTAB complexes, corresponding to a decrease in turbidity. Beyond c_2 , casein chains are saturated by DTAB molecules, and the turbidity remains constant. In this concentration range, the size of the new casein/DTAB complexes is larger than that of free casein micelles, which results in a higher turbidity than that in the absence of surfactant, as confirmed by DLS (see the next section). The values of c_1 and c_2 obtained here are found to agree with the results from ITC measurements.

Dynamic Light Scattering. DLS measurements were used to further investigate the mechanism of interaction between DTAB and casein. The distribution function of 2.0 mg/mL casein solution in the absence of DTAB is bimodal (data not shown). The fast mode represents the casein submicelles and monomers, and the slow mode characterizes the casein micelles.

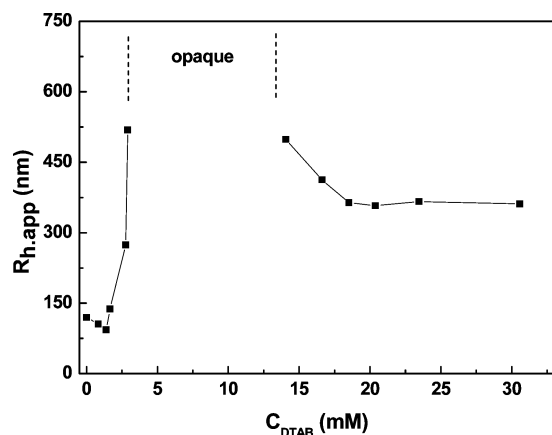


Figure 3. Relationship of the apparent hydrodynamic radii with DTAB concentration for 2.0 mg/mL casein and DTAB.

The relationship of the apparent hydrodynamic radii ($R_{h,app}$) of the slow modes, which represent the casein/DTAB complex, with the DTAB concentration is shown in Figure 3. As indicated by the turbidity, there are soluble casein/surfactant complexes at low and high DTAB concentrations. Since the DLS experiments cannot provide credible results when insoluble casein/DTAB complexes are formed, only the data at low and high DTAB concentrations are shown here. It is found that $R_{h,app}$ of casein micelles in the absence of surfactant is about 120 nm, which is consistent with literature values.^{15,16} At very low surfactant concentrations, $0 < c < 1.4$ mM, the increasing amount of the surfactant in solution leads to a decrease in $R_{h,app}$ of the casein micelles to a minimum. $R_{h,app}$ then increases sharply at DTAB concentration higher than 1.4 mM. At higher DTAB concentrations, $R_{h,app}$ decreases with DTAB concentration, reaching an asymptote of about 360 nm at the DTAB concentration of about 18 mM.

When we add DTAB to the casein solution, the negative charge of carboxylates at the casein micellar shell is neutralized, with the polar head of DTAB bound to the casein chains. Thus, the repulsion between the carboxylates is decreased, and the solubility of κ -casein is also decreased, resulting in the conformational change of κ -casein from extended to shrunken forms, which in turn leads to the decreased hydrodynamic radius of casein micelles. However, the decreased electrostatic repulsion between casein molecules leads to the more compact structure of casein micelles, and also the decrease of the hydrodynamic radius.

As discussed in the above section, the marked increase in $R_{h,app}$ is due to the low solubility of casein/DTAB complexes at DTAB concentrations higher than 1.4 mM, and the decrease in $R_{h,app}$ is due to the dissolution of the large insoluble casein/DTAB complexes at higher DTAB concentration. The binding of DTAB to casein is saturated, and $R_{h,app}$ remains constant when the DTAB concentration is higher than 18 mM. It can be found that the constant value of $R_{h,app}$ at DTAB concentrations higher than 18 mM is higher than that in the absence of surfactant, which can be explained by the following two factors. First, large casein/DTAB complexes only partially dissociate into smaller complexes. Second, the bound DTAB aggregates on the casein chains also lead to the increase in the size of casein/DTAB complexes.

Intrinsic Fluorescence Studies. Fluorescence experiments were also used to study the casein/DTAB complex. Among all the amino acid residues in proteins, tryptophan (Trp) has by far the highest fluorescence yield, and its fluorescence is strongly influenced by its environment because of the indole chro-

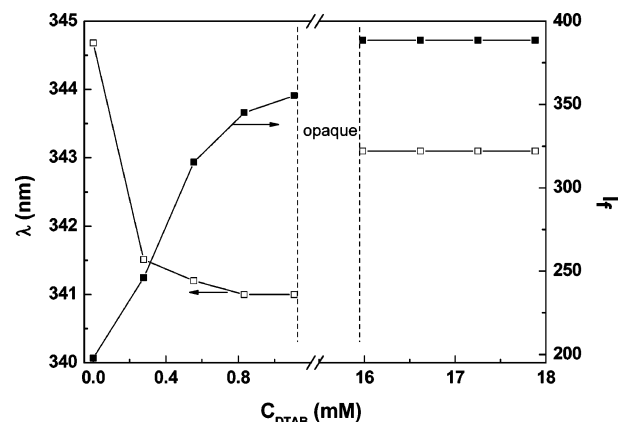


Figure 4. Plots of fluorescence maximum intensity (■) and emission wavelength (□) for 2.0 mg/mL casein against DTAB concentration.

mophore present in Trp. Casein consists mainly of α_{s1} - and β -casein. α_{s1} -casein contains two Trp residues at positions 164 and 199, and β -casein has a Trp residue at position 143. Thus, the three Trp residues are mainly located in a primarily hydrophobic domain of the casein micelle and can provide important information on the casein micelle structure.^{29,30}

As indicated by the turbidity, there are soluble casein/surfactant complexes with the initial binding of surfactants, and casein/surfactant complexes are dissociated again after the addition of more surfactants. Thus, we performed fluorescence experiments on native casein micelles and casein micelles mixed with DTAB at DTAB concentrations lower than 1.4 mM and higher than 16 mM. Between DTAB concentrations of 1.4 and 16 mM, fluorescence could not be conducted precisely because of the high turbidity of the system. Although the turbidity of the system with DTAB concentration of 16 mM is a little higher, the experiments show that the baseline is well enough to provide credible results.

The casein solution was selectively excited at 295 nm to avoid interference from the tyrosine residues.³¹ Figure 4 shows the influence of DTAB concentration on emission intensity (I_f) and maximum emission wavelength (λ_{max}). As shown in Figure 4, the sharp increase in I_f is accompanied by a blue shift in λ_{max} with the increase of DTAB concentration at DTAB concentrations lower than 1.4 mM. When the system becomes clear again, I_f and λ_{max} increases a little and then remain almost unchanged with further additions of DTAB.

Just as discussed above, the binding of DTAB monomers to casein micelles makes the structure of casein micelles more compact with the addition of DTAB at DTAB concentrations lower than 1.4 mM. Thus, the Trp residues are located at a more hydrophobic domain, which leads to a lower λ_{max} and a higher I_f . Beyond c' , the larger casein/DTAB complex redissolves. The electrostatic repulsion among more and more bound surfactant aggregates causes the structure of the new casein/DTAB complex to be looser, which makes the Trp residues be located at a more polar microdomain in casein/DTAB complexes and hence a higher λ_{max} .

It is noteworthy that the λ_{max} of Trp residues at high DTAB concentration does not change much compared with that in the absence of DTAB. Clearly, Trp residues are not exposed to the aqueous phase, which indicates that the hydrophobic domain of casein micelles is not disrupted completely at high DTAB concentrations.

Pyrene and ANS Fluorescence Studies. Pyrene is an excellent probe of local environment polarity changes. The intensity ratio of the first peak to the third peak (I_1/I_3) of the

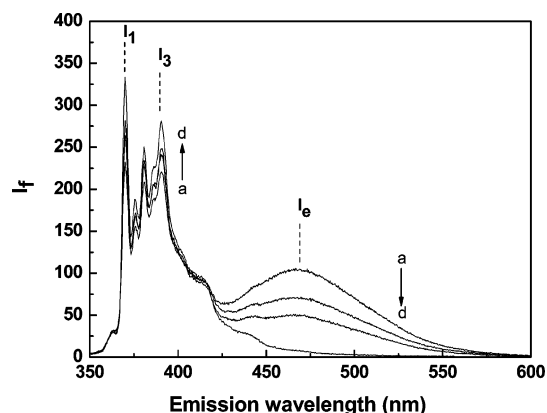


Figure 5. Effect of DTAB on the fluorescence emission spectra of pyrene in casein solution (2.0 mg/mL). C_{DTAB} (mM): (a) 0, (b) 0.277, (c) 0.555, (d) 16.

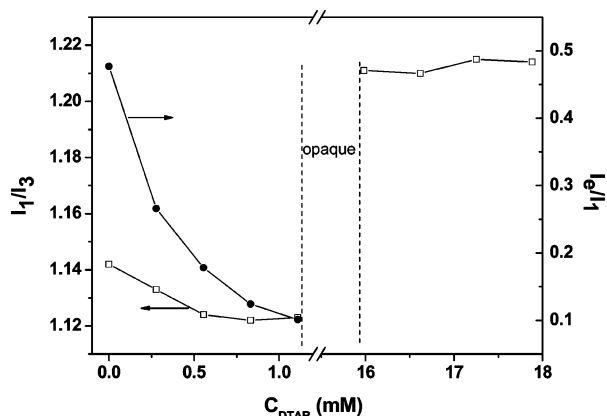


Figure 6. Plots of I_1/I_3 (□) and I_e/I_1 (■) against DTAB concentration in the presence of 2.0 mg/mL casein.

fluorescence spectrum of pyrene shows the microenvironmental polarity where the probe exists.³² Furthermore, an excited monomer can encounter a ground-state pyrene to form an excimer, which gives a broad band at about 450 nm. The ratio of the maximum emission intensity of the excimer (I_e) to the monomer (I_1) for pyrene, I_e/I_1 , can be used to judge the efficiency of excimer formation, which can provide further information about the hydrophobic domain in the micelle.³³

Figure 5 shows the fluorescence spectra of pyrene in the casein solution with different DTAB concentrations. Figure 6 shows the effect of DTAB concentration on the I_1/I_3 and I_e/I_1 ratio. As can be seen, the intensity ratio has a value of 1.14 in the absence of surfactants, which indicates that pyrene molecules reside in a hydrophobic domain in casein micelles. I_1/I_3 decreases at DTAB concentrations lower than 1.4 mM, increases obviously, and then remains unchanged at DTAB concentrations higher than 16 mM with the addition of DTAB.

The more compact structure of casein micelles makes the pyrene molecules be located at a more hydrophobic domain, resulting in a lower I_1/I_3 with the addition of DTAB below DTAB concentrations of 1.4 mM. The looser structure of the new casein/DTAB complex leads the micropolarity around the pyrene molecules to be higher, hence a higher ratio of I_1/I_3 when the casein/DTAB system becomes clear again. Moreover, the ratio I_1/I_3 (1.21) for casein/DTAB complexes at high DTAB concentrations is lower than the ratio I_1/I_3 (1.35) for pure DTAB micelles. Thus, the hydrophobic microdomains of casein/DTAB complexes at high DTAB concentrations are more hydrophobic than pure DTAB micelles.

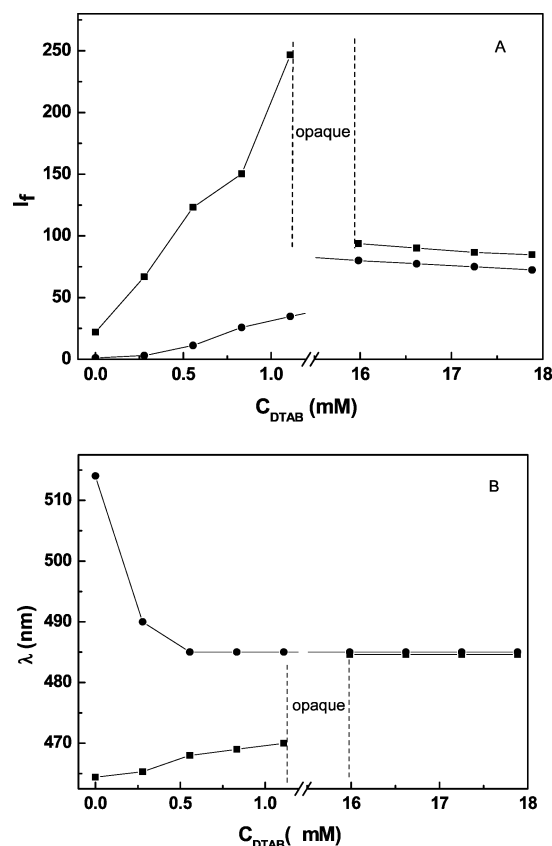


Figure 7. Plots of the fluorescence maximum intensity (A) and emission wavelength (B) of ANS against DTAB concentration in the absence (●) and presence of (■) 2.0 mg/mL casein.

As shown in Figures 5 and 6, I_e and I_e/I_1 drop significantly at DTAB concentrations lower than 1.4 mM with the addition of DTAB. This indicates that the pyrene molecules located at the hydrophobic domain in casein micelles are stacked in a favorable configuration for the excimer formation. However, the more compact structure of casein micelles upon the addition of the DTAB makes the pyrenes be stacked in an unfavorable configuration for pyrene excimer formation, hence a lower I_e .

Because pyrene is a neutral hydrophobic probe, it is not influenced by the cationic headgroup of DTAB bound on casein micelles. The extrinsic fluorescence measurements have also been performed with another probe, ANS, which possesses an anionic sulfonate group. The quantum yield of ANS is about 0.004, and the emission maximum is 520 nm in water, whereas it has a strong emission in nonpolar organic solvents and a low λ_{max} , suggesting that the changes in ANS fluorescent properties are mainly due to the changes in the polarity of the dye microenvironment.^{34,35}

The effects of DTAB concentration on I_f and λ_{max} of ANS in the absence and presence of casein are shown in Figure 7. Figure 7 shows that the decrease of the I_f is accompanied by a red shift in λ_{max} with the increase in DTAB concentration at DTAB concentrations lower than 1.4 mM in casein solution. In this concentration region, the effect of DTAB on I_f and λ_{max} in the presence of casein micelles is very much different from that in the absence of the casein micelle. When the system becomes clear again, I_f decreases, and λ_{max} increases obviously, and then remains almost unchanged with the addition of DTAB. In this concentration region, I_f and λ_{max} in the presence of casein are very similar to that in the absence of casein.

The small λ_{max} of ANS in the casein solution in the absence of DTAB shows that portions of ANS molecules are located at

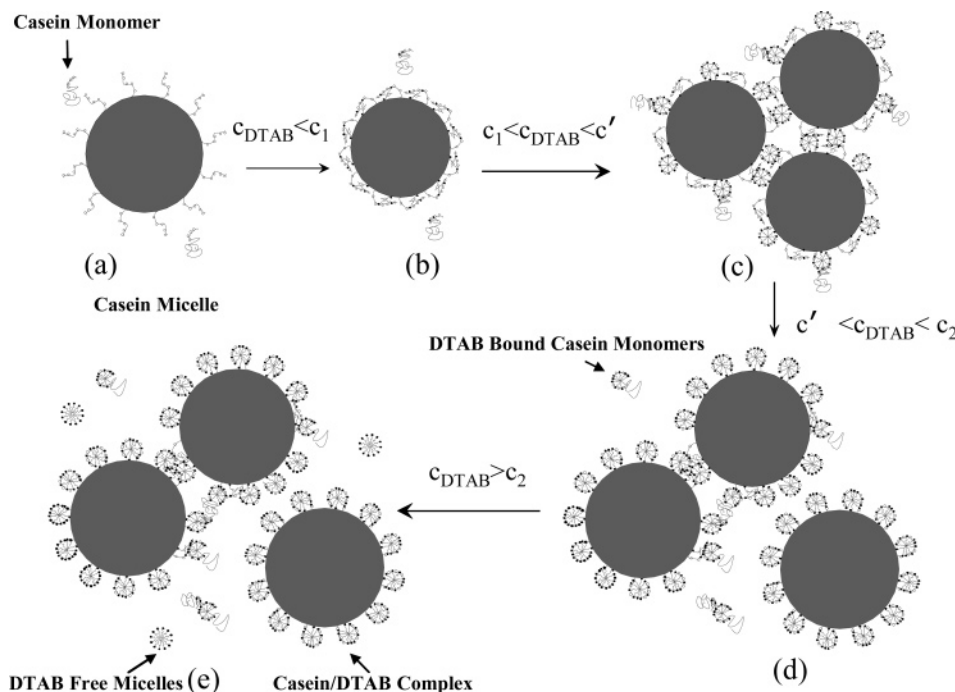


Figure 8. Schematic diagram describing the binding interactions between DTAB and 2.0 mg/mL casein at different DTAB concentrations.

the hydrophobic domain of casein micelles. DTAB molecules bind to the negative sites on the casein micelle shell upon the addition of DTAB. Since ANS is negatively charged, the electrostatic attraction between the polar head of DTAB and ANS causes ANS molecules located at the hydrophobic domain of casein micelles to move toward the casein micelle shell, which leads to the increase in microenvironment polarity around those ANS molecules, leading to a higher λ_{\max} . At the same time, some portions of ANS molecules located in the aqueous solution are transferred into the casein micelle shell because of the electrostatic interaction between ANS and DTAB, which causes more ANS molecules to be located at more hydrophobic domains, resulting in the sharp increase in I_f . When the system becomes clear again, more DTAB aggregates bind on the casein micelle shell, and almost all ANS molecules transfer into the micelle-like DTAB aggregates because of the strong electrostatic attraction, which causes the microenvironment around ANS molecules in the presence and in the absence of casein to be similar. Therefore, λ_{\max} and I_f of ANS in the presence of caseins is very similar to that in the absence of casein at DTAB concentrations higher than 16 mM. Our results show that electrostatic interaction plays an important role in the binding of ANS to the casein/DTAB complex and that the hydrophobic affinity is a minor interaction among ANS and casein/DTAB complexes, which is consistent with the results of Matulis and Lovrien.³⁶

Binding Mechanism. Taking all of the above results for the casein/DTAB system into consideration, a simple model of interaction between DTAB and the casein is depicted in Figure 8. In the absence of DTAB, casein micelles coexist with casein monomers (or submicelles) in the 2.0 mg/mL casein solution, as shown in Figure 8a. For simplicity, only casein micelles and monomers are given in the figure. At DTAB concentrations lower than c_1 (1.4 mM), the cationic headgroups of the surfactant individually bind to the negatively charged amino acid sites on the casein chains because of electrostatic attraction (Figure 8b), which results in an increase in ΔH_{obs} . At the same time, the structure of casein micelles becomes more compact because of the decrease in the net negative charge of the casein micelle

shell and hence a decrease of the casein micelle's hydrodynamic radius. Therefore, the Trp residues and pyrene are located in a more hydrophobic domain. On the contrary, the anionic probe ANS senses a more hydrophilic microenvironment because of the electrostatic action between ANS and DTAB. When the DTAB concentration exceeds c_1 , the casein bound surfactant aggregates result in the formation of large insoluble casein/surfactant complexes (Figure 8c) because of the marked electrical neutralization of the negative charge of casein micelles by cationic DTAB. This leads to the sharp increase in the turbidity of the system beyond c_1 . Beyond c' , the net positive charges on the complexes due to the binding by more cationic surfactant molecules lead to a redissolution of the complexes (Figure 8d), corresponding to the formation of the new casein/DTAB complexes. Furthermore, the structure of the new casein/DTAB complexes is looser because of the electrostatic repulsion between the bound DTAB aggregates. Thus, the Trp residues and pyrene are located in a more hydrophilic microenvironment. At a DTAB concentration of 18 mM (c_2), all of the caseins are saturated by DTAB aggregates, and free DTAB micelles appear in solution (Figure 8e).

Conclusions

The complexing of 2.0 mg/mL casein with the cationic surfactant DTAB has been studied. DTAB monomers bind to the negatively charged amino acid sites on casein chains (including casein micelles, submicelles, and monomers) by electrostatic attraction below c_1 , which makes the structure of casein micelles become more compact because of the decrease in the net negative charge of the casein micelle shell. When the surfactant concentration reaches c_1 , the micellization of casein bound surfactant occurs, resulting in the formation of insoluble casein/surfactant complexes. The further addition of DTAB leads to the redissolution of the casein/DTAB complexes because of the net positive charge on complexes. The structure of the new casein/DTAB complex is looser because of the highly bound DTAB aggregates. Electrostatic interaction plays an important role in the binding of ANS to the casein/DTAB

complex. It is believed that the above findings provide new insights into the form–function relationship of casein micelles modulated by the cationic surfactant, which will broaden the application range of casein micelles in food, cosmetic, and medical domains.

Acknowledgment. This work was supported by the National Nature Science Foundation of China (20633010).

References and Notes

- (1) Lee, L. T.; Jha, B. K.; Malmsten, M.; Holmberg, K. *J. Phys. Chem. B* **1999**, *103*, 7489–7494.
- (2) Meier, W.; Ramsden, J. J. *J. Phys. Chem.* **1996**, *100*, 1435–1438.
- (3) De Oliveira, V. A.; Tiera, M. J.; Neumann, M. G. *Langmuir* **1996**, *12*, 607–612.
- (4) Thuresson, K.; Lindman, B. *J. Phys. Chem. B* **1997**, *101*, 6460–6468.
- (5) Schillen, K.; Anghel, D. F.; da Graca Miguel, M.; Lindman, B. *Langmuir* **2000**, *16*, 10528–10539.
- (6) Hoff, E.; Nystrom, B.; Lindman, B. *Langmuir* **2001**, *17*, 28–34.
- (7) Dai, S.; Tam, K. C.; Li, L. *Macromolecules* **2001**, *34*, 7049–7055.
- (8) Goddard, E. D. *J. Colloid Interface Sci.* **2002**, *256*, 228–235.
- (9) Ritacco, H.; Kurlat, D.; Langevin, D. *J. Phys. Chem. B* **2003**, *107*, 9146–9158.
- (10) Jain, N.; Trabelsi, S.; Guillot, S.; McLoughlin, D.; Langevin, D.; Letellier, P.; Turmine, M. *Langmuir* **2004**, *20*, 8496–8503.
- (11) Nizri, G.; Magdassi, S.; Schmidt, J.; Cohen, Y.; Talmon, Y. *Langmuir* **2004**, *20*, 4380–4385.
- (12) Turro, N. J.; Lei, X. G. *Langmuir* **1995**, *11*, 2525–2533.
- (13) Bai, G. Y.; Nichifor, M.; Lopes, A.; Bastos, M. *J. Phys. Chem. B* **2005**, *109*, 518–525.
- (14) Castro, E.; Taboada, P.; Barbosa, S.; Mosquera, V. *Biomacromolecules* **2005**, *6*, 1438–1447.
- (15) Garnier, C.; Michon, C.; Durand, S.; Cuvelier, G., D.; J. L.; Launay, B. *Colloids Surf., B* **2003**, *31*, 177–184.
- (16) Euston, S. R.; Horne, D. S. *Food Hydrocolloids* **2005**, *19*, 379–386.
- (17) Pan, X. Y.; Mu, M. F.; Yao, P.; Jiang, M. *Biopolymers* **2006**, *81*, 29–38.
- (18) Horne, D. H. *Curr. Opin. Colloid Interface Sci.* **2006**, *11*, 148–153.
- (19) Tuinier, R.; Rolin, C.; De Kruif, C. G. *Biomacromolecules* **2002**, *3*, 632–638.
- (20) Verma, A.; Simard, J. M.; Rotello, V. M. *Langmuir* **2004**, *20*, 4178–4181.
- (21) Ausar, S. F.; Bianco, I. D.; Castagna, L. F.; Alasino, R. V.; Beltramo, D. M. *J. Agric. Food Chem.* **2003**, *51*, 4417–4423.
- (22) Anema, S. G.; Li, Y. M. *J. Agric. Food Chem.* **2003**, *51*, 1640–1646.
- (23) Marozzini, A.; De Kruif, C. G. *Food Hydrocolloids* **2000**, *14*, 391–394.
- (24) Wang, X. Y.; Li, Y. J.; Li, J. X.; Wang, J. B.; Wang, Y. L.; Guo, Z. X.; Yan, H. K. *J. Phys. Chem. B* **2005**, *109*, 10807–10812.
- (25) Wang, C.; Tam, K. C. *J. Phys. Chem. B* **2004**, *108*, 8976–8982.
- (26) Gianni, P.; Barghini, A.; Bernazzani, L.; Mollica, V.; Pizzolla, P. *J. Phys. Chem. B* **2006**, *110*, 9112–9121.
- (27) Kujawa, P.; Raju, B. B.; Winnik, F. M. *Langmuir* **2005**, *21*, 10046–10053.
- (28) Dai, S.; Tam, K. C. *J. Phys. Chem. B* **2001**, *105*, 10759–10763.
- (29) Michael, H. A.; Harold, M. F. J.; Markus, W. G. *Biochim. Biophys. Acta* **1999**, *1431*, 410–420.
- (30) Harold, M. F. J.; Wickham, E. D.; Unruh, J. J.; Qi, P. X.; Hoargland, P. D. *Food Hydrocolloids* **2001**, *15*, 341–354.
- (31) Li, Y. J.; Wang, X. Y.; Wang, Y. L. *J. Phys. Chem. B* **2006**, *110*, 8499–8505.
- (32) Christine, K. B.; Jean, D.; Shan, Y. F.; Jeremy, B.; Chen, P. J. *Am. Chem. Soc.* **2004**, *126*, 7522–7532.
- (33) Daisy, S.; Vasanthy, N.; Cyril, M. K.; Robert, O. R. *Biochemistry* **2000**, *39*, 6594–6601.
- (34) Manderson, G. A.; Hardman, M. J.; Creamer, L. K. *J. Agric. Food Chem.* **1999**, *47*, 3617–3627.
- (35) Poklar, N.; Lah, J.; Salobir, M.; Macek, P.; Vesnaver, G. *Biochemistry* **1997**, *36*, 14345–14352.
- (36) Matulis, D.; Lovrien, R. E. *Biophys. J.* **1998**, *74*, 422–429.

BM7006136